Oligo DNA-based quantum dot (QD) single-particle tracking for multicolor single-molecule imaging

Shigeo Sakuragi[1], Naoki Kato[1], Tomoya Uchida[1], Taro Katagiri[1], Miyu Enomoto[1], Rie Kato[1], Hideaki Yoshimura[2], Chisato Oyama[1], Iona Katayama[1], Ayano Chikuma[1], Yuji Teramura[3, 4], and Hiroko Bannai[1]

[1] *Department of Electrical Engineering and Biosciences, School of Advanced Science and Engineering, Waseda University, Shinjuku-Ku, Tokyo 162-0056, Japan*

[2] *Department of Chemistry, School of Science, The University of Tokyo, Bunkyo-ku, Tokyo 113-0033, Japan*

[3] *Department of Bioengineering, Graduate School of Engineering, The University of Tokyo, 7-3-1 Hongo, Bunkyo-ku, Tokyo, 113-8656, Japan*

[4] ***Current address**: Cellular and Molecular Biotechnology Research Institute (CMB), National Institute of Advanced Industrial Science and Technology (AIST), AIST Tsukuba Central 5, 1-1-1 Higashi, Tsukuba, Ibaraki 305-8565, Japan*

Quantum dot single-particle tracking (QD-SPT), a powerful tool for analyzing membrane domains that are critical to various cellular processes, is widely used in membrane molecular dynamics research. QDs, which possess both a broad excitation range and a narrow emission bandwidth, are inherently suited for multicolor imaging at various wavelengths. However, applying multicolor QD-SPT with multiple biomolecular targets has been challenging due to the limited methods for specifically conjugating QDs to biomolecules. Here, we propose a DNA hybridization-based QD labeling method that generates several specific interactions based on sequence. QD fused with 20-mer oligo DNA specifically labeled membrane lipid 1,2-dipalmitoyl-sn-glycero-3-phosphatidylethanolamine (DPPE) covalently bound to complementary oligo DNA, forming a stable label that is suitable for SPT. The combination of polyA–polyT sequence as the linker oligo caused more QDs to fuse to DPPE compared with a random sequence linker. Oligo DNA-based QD-SPT accurately reflected the diffusion dynamics of DPPE measured using the single-fluorescence tracking technique and was compatible with conventional QD-SPT utilizing secondary antibody Fab. Using different pairs of oligo DNA sequences, we successfully achieved multicolor QD-SPT that distinguishes a lateral diffusion of DPPE and a membrane protein, $GABA_A$ receptor, within the same cell. The oligo DNA-based QD labeling method developed in this study is anticipated to substantially advance simultaneous multicolor QD-SPT of different living cell membrane molecules specific to DNA sequences.

Keywords: quantum dot, single-particle tracking, multicolor imaging, membrane molecule, diffusion

◀ ***Significance*** ▶

Quantum dot single-particle tracking (QD-SPT) is a powerful approach for investigating membrane dynamics; however, the limited conjugation methods available hinder multicolor labeling. This study introduces a DNA hybridization-based labeling strategy, where QDs conjugated with 20-mer oligos that specifically bind to complementary oligo-tagged lipids or antibodies. PolyA–polyT linkers improved labeling efficiency compared with random sequences. This method accurately captured 1,2-dipalmitoyl-sn-glycero-3-phosphatidylethanolamine (DPPE) diffusion, matched conventional QD-SPT, and enabled simultaneous multicolor tracking of DPPE and $GABA_A$ receptors in the same cell. This oligo-DNA-based approach enables multicolor QD-SPT of distinct membrane proteins.

Corresponding author: Hiroko Bannai, Waseda University, Shinjuku, Tokyo 162-0056, Japan. ORCID iD: https://orcid.org/0000-0002-0951-488X, e-mail: hiroko.bannai@waseda.jp

Introduction

In the fluid-mosaic model proposed by Singer and Nicolson, biological membranes demonstrate fluid-like properties, in which membrane proteins and lipids that are embedded in the lipid bilayer undergo lateral diffusion across the plasma membrane [1]. However, high-resolution analyses at the sub-millisecond timescale have revealed that even lipid molecules that diffuse freely are transiently confined within compartments of approximately 13–100 nm in size, based on the actin cytoskeleton and transmembrane proteins anchored to it. Lipid molecules display compartmentalized diffusion, characterized by restricted motion within individual compartments and occasional hopping between adjacent compartments [2] [3]. Furthermore, specific membrane proteins are localized in the membrane region on the nanometer to micrometer scale, generating functional membrane domains [4]. These domains are developed through fine regulation and restriction of lateral diffusion of membrane molecules and play crucial roles in a wide array of cellular processes, including signal transduction, synaptic transmission, and immune responses. For example, neurotransmitter receptors accumulate at the synapse, which serve as the fundamental units of inter-neuronal communication, and the number of receptors at the synapse, ultimately, the efficacy of synaptic transmission, is regulated via lateral diffusion constraints caused by interactions between receptors and scaffold proteins [5]. Further, transmembrane proteins and cytoskeletons restrict the lateral diffusion of membrane lipids in the axon initial segment of neurons, underlying the physical compartmentalization between neuronal input and output domains [6]. Observations of membrane molecule dynamics are crucial to understanding such self-organizing principles of plasma membranes and revealing the molecular mechanisms underlying their physiological functions.

Single-molecule imaging enables the observation of the dynamics of individual molecules, facilitating not only the assessment of ensemble behavior but also detailed information about the behavior of molecules in confined microdomains, stochastic movements, and heterogeneity within molecular populations. Single-particle tracking (SPT) is one of the representative methods in single-molecule imaging, in which probes are specifically conjugated to target molecules in live cells, causing the high-precision tracking of particle positions [7]. Among the SPT methods that use diverse probes, quantum dot (QD)-SPT has become a widely used approach for investigating the dynamics of membrane molecules in neurons. QDs are semiconductor nanocrystals that serve as fluorescent probes, which overcome limitations associated with organic fluorophores caused by their superior brightness and long fluorescence lifetimes [5]. Furthermore, their high brightness and significant Stokes shift provide an excellent signal-to-noise ratio (SNR), enabling more straightforward and higher-resolution analysis of fluorescence images compared with organic dyes [8]. However, QDs still have certain limitations, as the relatively large size of QD bioconjugates hinders access to spatially restricted regions, such as synaptic clefts, due to physical confinement [9] [10]. The blinking of QDs, i.e., intermittent fluorescence emission, hinders continuous tracking and quantitative analysis [11]. However, the optical advantages of QDs, particularly their high SNR, which helps improve spatial resolution, outweigh these drawbacks. Hence, QD-SPT has been extensively adopted in neuroscience research to investigate membrane molecule dynamics at the single-molecule level.

The most distinctive feature of QDs is that their fluorescence emission wavelength is precisely identified based on their particle size, leading to sharp and narrow emission spectra [12]. With their broad excitation range and narrow emission bandwidth, QDs are inherently well-suited for multicolor imaging of various wavelengths. Indeed, studies that used fixed tissues and cells reported multicolor imaging employing QDs [13] [14] [15]. Despite developing QD-SPT over 20 years ago, reports that utilize QDs for multicolor imaging, particularly those involving labeling of multiple molecular species with QDs of distinct emission wavelengths, are limited. The lack of robust methods for specifically labeling different target molecules in living cells with QDs with different wavelengths of emission is one of the primary reasons. Currently, the commonly used QD labeling method employs the specific interaction between the primary antibodies and secondary antibodies or biotin–avidin interactions. However, these methods involve a small number of combinations of specific molecular interactions, which limits the options for multicolor imaging that simultaneously targets multiple different molecules. Therefore, novel QD-labeling strategies need to be developed to expand the applicability of multicolor QD-SPT in the same cell.

In this study, we propose a QD-labeling method based on DNA hybridization, which generates several specific interactions based on the sequence. DNA-PAINT, one of the super-resolution imaging methods, uses the transient hybridization of complementary DNA strands between a dye-labeled probe and a target. In DNA-PAINT, the sequences and lengths of single-stranded oligo DNA (ssDNA) are precisely designed to enable repeated binding and unbinding events, and the fusion of ssDNA to antibodies permits single-molecule localization imaging of

specific proteins [16]. Here, we adapted the concept of DNA-PAINT and *in situ* hybridization to SPT. We used the specific and stable hybridization between complementary DNA strands to achieve stable conjugation between membrane molecules and QDs, enabling sequence-specific targeting of distinct membrane molecules with QDs of defined emission properties. Utilizing this approach, we demonstrate a practical method for multicolor QD-SPT in the same cell, wherein multiple molecular species, the phospholipid and the neurotransmitter receptor, are labeled with QDs through 20-mer DNA hybridization, each emitting at different wavelengths.

Materials and methods

Primary culture of rat hippocampal neurons

In this study, all experiments were conducted following the guidelines approved by the Animal Experimentation Committee of Waseda University. Primary hippocampal neurons were prepared as previously described [17]. In brief, hippocampi were dissected from embryonic day 20 (E20) Wistar/ST rats (Japan SLC) and treated with 0.125% trypsin (Sigma-Aldrich) and 0.025 w/v% DNase (Sigma-Aldrich). The tissue was then dissociated in the plating medium, composed of the minimum essential medium (MEM; Thermo Fisher Scientific) supplemented with 2% MACS NeuroBrew-21 (Miltenyi Biotec), 2 mM L-glutamine (Nacalai Tesque), 1 mM sodium pyruvate (Nacalai Tesque), and 5 units/mL of penicillin and 5 μg/mL of streptomycin (Nacalai Tesque). Dissociated cells were seeded at a density of 1.4×10^5 cells per well on an 18-mm polyethyleneimine-coated glass coverslip, and cultured in a CO_2 incubator (37°C, 5% CO_2). Four days after plating, the culture medium was replaced with the maintenance medium, the neurobasal-A medium (Thermo Fisher Scientific), supplemented with 2% MACS NeuroBrew-21, 2 mM L-glutamine, and penicillin (5 units/mL)/streptomycin (5 μg/mL). Cultures were maintained at 37°C in a CO_2 incubator until the experiments were performed at 14 days *in vitro* (DIV14) or later.

Membrane molecule labeling using ssDNA

We prepared 20 base-pair ssDNA probes comprising one pair of complementary poly sequences (polyA and polyT) and two pairs of complementary random sequences (random1S and random1AS, random2S and random2AS). Table S1 shows the sequence. For the QD-SPT of phospholipids with ssDNA-conjugated QDs, we prepared the 1,2-dipalmitoyl-sn-glycero-3-phosphatidylethanolamine (DPPE) tagged with ssDNA at the hydrophilic head group (ssDNA–DPPE) (Figure 1). As previously described, ssDNA was attached to maleimide-poly(ethylene glycol)-conjugated phospholipid DPPE through a thiol–maleimide reaction (Supplementary Figure S1A) [18]. In brief, DPPE and α-N-hydroxysuccinimidyl-ω-maleimidyl poly(ethylene glycol) (NHS-PEG-Mal, Mw: 5000) were combined to produce Mal-PEG-DPPE. Thiolated-labeled ssDNAs to the 5' end were then reacted with Mal-PEG-DPPE to obtain the ssDNA–DPPE and maintained in the phosphate-buffered saline (PBS). Further, DPPE was conjugated with ssDNA via copper-free click chemistry through dibenzocyclooctyl (DBCO)–azide conjugation (ssDNA–DBCO–DPPE, Supplementary Figure S1B) [19] [20]. DPPE–PEG(2000)–azide (10 μM; Avanti) was reacted with 5' DBCO-C6-N_2-PolyA(20) (1 μM; Nihon Gene Research Laboratories) in PBS for 60 min at room temperature.

Moreover, ssDNA and QD conjugates (ssDNA–QD) were prepared by mixing Qdot 655 streptavidin conjugate (1 μM; QD655; Thermo Fisher Scientific), ssDNA labeled with biotin at the 5' end (10 μM), and Qdot Binding Buffer (QBB; 2.62 mM sodium tetraborate decahydrate [Wako], 39.5 mM boric acid [Nacalai Tesque], 2 w/v% bovine serum albumin [Sigma-Aldrich], 0.05 w/v% sodium azide) at a volume ratio of 1.0:0.5:8.5, followed by overnight incubation at 4°C. QD605 (Thermo Fisher Scientific) conjugated with ssDNA as described above was used for simultaneous labeling of multiple membrane proteins in parallel with ssDNA–QD655. The imaging medium, MEM without phenol red (Thermo Fisher Scientific), supplemented with 20 mM HEPES (Sigma Aldrich), 2 mM glutamine, 1 mM sodium pyruvate, and 33 mM glucose (Nacalai Tesque), was used for the dilution and the incubation of lipid and antibody, cell washing, and live-cell imaging. QBB was supplemented with 215 mM of sucrose (QBB-suc) to adjust the osmolarity when QDs were incubated with neurons.

To incorporate ssDNA–DPPE into the plasma membrane, ssDNA–DPPE (5 μg/mL) was incubated with primary cultured rat hippocampal neurons for 5 min. After washing, the coverslips were incubated with 0.25 μM ssDNA–QD in QBB-suc for 1 min, followed by washing and imaging in the imaging medium. Labeling processes, which include lipid, antibody, and QD incubation, were performed in a humid chamber placed on a heating plate maintained at 37°C [21].

For labeling $GABA_A$ receptors ($GABA_ARs$) with ssDNA, we utilized a custom-made antibody that targets the extracellular domain of the γ2 subunit of $GABA_AR$ [22] conjugated with polyA (ssDNA–Ab; Figure 1). The antibody was conjugated to ssDNA at a 1:5 molar ratio employing the Oligonucleotide Conjugation Kit (Abcam,

ab218260), which targets lysine residues via an amine-reactive ester. Endogenous $GABA_AR$ in cultured rat hippocampal neurons were labeled with ssDNA by incubating with 0.004 mg/mL of ssDNA–$GABA_AR$ antibody for 5 min, followed by incubation with 0.25 μM ssDNA–QD in QBB-suc for 1 min in a humid chamber.

Conventional QD labeling using Fab fragment antibody

$GABA_AR$ labeling using Fab fragment antibody as a linker for QD (conventional labeling) was performed according to previous reports [21] [23]. Rat primary hippocampal neurons were incubated with a custom-made anti-$GABA_AR$ γ2 subunit antibody that targets the extracellular domain (0.004 mg/ml, 5 min) followed by incubation with biotinylated Fab fragment antibody (10 μg/ml, 5 min; Biotin-Fab, Jackson ImmunoResearch). After washing, $GABA_ARs$ were labeled via biotin–avidin binding by incubation with 1 μM QD655 or QD605 in QBB-suc at 37°C for 1 min.

QD-SPT data acquisition

QD-SPT was conducted using an inverted microscope (IX73, Olympus) equipped with multi-wavelength LED illumination (niji, Bluebox Optics), an oil-immersion objective lens (×60, NA 1.42, Olympus), and filter sets for QD wavelength, i.e., an excitation filter (450/70 nm, e.g., Semrock, Rochester, NY; BrightLine® single-band band-pass filter #FF01-450/70-25), dichroic beam splitters (DM) and emission filter (EM) based on each QD emission wavelength (for Qdot655: 655/15 nm #FF01-655/15-25, DM #FF640-FDi01-25 × 36; for Qdot605: 605/15 nm #FF01-605/15-25, DM #FF593-Di03), and the EM-CCD camera (ImagEM C9100-13, Hamamatsu Photonics). MetaVue software (Molecular Devices) was used to control the excitation illumination and the EM-CCD camera. A total of 200 consecutive frames of QD images were recorded at a frequency of 13 Hz with an exposure time of 75 ms. During observation, the specimen and the microscope stage were maintained at 37°C using a heating system (Tokai Hit). In the DNase experiment, 0.05 w/v% DNase (Sigma-Aldrich) in Hank's balanced salt solution (Nacalai Tesque) was added to the observation chamber on the microscope stage and left for 3 min. Images were then acquired in the same field of view after DNase administration.

Single-fluorescence tracking for DPPE

The ATTO647–DPPE (ATTO-TEC GmbH, AD647-151) was inserted in the cultured neurons by incubating the coverslips with 0.1 μM ATTO647–DPPE diluted in the imaging medium for 10 min, within the humid chamber placed in a CO_2 incubator. After washing three times, the coverslip was mounted in the observation chamber and immersed in the imaging medium for observation.

Total internal reflection fluorescence microscopy (TIRFM) was used for single-molecule fluorescence imaging of organic dye ATTO647 [24], based on an inverted microscope (IX81, Olympus) equipped with 640-nm diode laser (CUBE, Coherent Inc.), 405/488/561/635-nm band excitation filter (Semrock Inc.), Dichroic mirror (FF662, Semrock Inc.), 697/58-nm band-pass filter (Semrock Inc.), EM-CCD camera (ImagEM, Hamamatsu Photonics), and an oil-immersion objective lens (×100, NA 1.49, Olympus). The imaging was performed in 256 × 256-pixel subarray mode, recording 200 frames at 30 Hz (33 ms/frame), at the surface and the bottom focal planes in the same field of view.

Tracking analysis of QD and organic dyes

A tracking analysis of QD-SPT was conducted using TI Workbench as previously described [21][25]. The center of each QD spot was defined based on cross-correlation of the fluorescent spots with a Gaussian model with a point spread function. QD-trajectories are automatically assembled by linking the centers of fluorescent spots. Only QDs with blinking were considered for the analysis to ensure that they are single particles (Dahan et al., 2003), with the trajectories with > 30 points used for further analysis. The mean squared displacement (MSD) was calculated from the coordinates of reconstructed trajectories. The MSD-Δt curve, which plots MSD versus time (Δt), was obtained using the following equation (1) [26]:

$$MSD(n\Delta t) = \frac{1}{N-n}\sum_{i=1}^{N-n}[(x((i+n)\Delta t) - x(i\Delta t))^2 + (y((i+n)\Delta t) - x(i\Delta t))^2] \quad (1)$$

where Δt denotes the acquisition time (75 ms), N indicates the total number of frames, n represents the frame number, and i denotes the positive integers. The diffusion coefficient (*D)* of QDs was obtained by fitting the first 1–4 points without origin of the MSD-$n\Delta t$ curves with the following equation (2):

$$MSD(n\Delta t) = 4Dn\Delta t \quad (2)$$

QDs with diffusion coefficients D of < 0.0004, equivalent to D of QDs adhered on the coverslips, were defined as "immobile" QDs [21].

Single-fluorophore tracking (SFT) images were filtered using the dilate (circle, 4 pixels) function in MetaMorph (Molecular Devices) to reduce spike-like noise, and the trajectories were composed employing TI Workbench software. To ensure single-molecule fluorescence, the analysis included only bright spots that disappeared in a single step during recording. The diffusion coefficients were calculated for trajectories tracked for more than 10 consecutive frames.

Statistics

Complementary binding by the four ssDNA–QDs was compared using a one-way analysis of variance with a post hoc Tukey HSD test. The number of QDs before and after DNase application was compared using a Wilcoxon signed-rank test. A Kolmogorov–Smirnov test was used to perform the cumulative distribution of the diffusion coefficient. A Mann–Whitney *U*-test was used for other statistical analyses. The figure illustrates the *P*-values. Sample size (N) for each experiment is described in the figure legend. Each experiment utilized at least three independent culture batches.

Result

QD Labeling of Membrane Molecules depending on annealing between complementary ssDNAs

First, we investigated whether the phospholipid DPPE tagged with ssDNA (ssDNA–DPPEs) was specifically labeled with QDs conjugated with ssDNA (ssDNA–QDs) with a complementary sequence through the hybridization. The 20-mer oligo DNA, composed of identical bases or random sequences, was developed as ssDNA sequences (Supplementary Table S1) and added to QDs and target molecules. DPPEs conjugated with polyA ssDNA (polyA–DPPE) via the thiol–maleimide reaction (Supplementary Figure S1A) were inserted into the plasma membrane of primary rat hippocampal neurons and incubated with QDs conjugated with either polyA or polyT sequences (Figure 2A). QDs with polyA (polyA–QDs), carrying the same sequence as the ssDNA on the DPPE, did not remain on the surface of the neurons, whereas QDs with polyT (polyT–QDs), which carry the complementary sequence, were observed on the neurons (Figure 2B). The median number of QDs bound to neurons per image was 1 for polyA–QDs, whereas that for polyT–QDs was significantly higher at 241 per image (Figure 2C, Supplementary Table S2). Comparable to the result of polyA–DPPEs, the DPPE tagged with polyA by the copper-free click chemistry through the DBCO–azide reaction (polyA-DBCO-DPPE, Figure S1B) was targeted by polyT–QDs, but not by polyA–QDs (Supplementary Figures S1C, S1D), indicating that the linker between the DPPE and the ssDNA does not affect the DNA hybridization. PolyA–QDs labeled the plasma membrane of neurons incubated with polyT–DPPE, whereas ssDNA–QD did not bind to neurons without polyT–DPPE (Supplementary Figures S2A, S2B). Furthermore, polyA–DPPE was rarely targeted with ssDNA–QD that carries two random sequences, random 1AS and random 2AS (Supplementary Figures S2C, S2D), indicating the high dependence of QD labeling via ssDNA on the DNA sequence complementarity. To further confirm the binding specificity of QD labeling with ssDNA, we inserted a random ssDNA sequence-conjugated DPPE (random1S–DPPE) into the plasma membrane of cultured neurons and evaluated whether QDs with four different ssDNA sequences (polyA, polyT, random1AS, and random2AS) could bind to random1S–DPPE (Figure 2D). QDs with polyA, polyT, or random2AS, all of which are not complementary to random1S, did not remain on the cell surface. In contrast, a substantial amount of QDs with the complementary sequence random1AS bound to random1s–DPPE (Figure 2E, Supplementary Table S2). Statistical analysis revealed that random1AS–QDs were significantly more observed in the plasma membrane (Figure 2F, Table S2). These results indicate that hybridization between 20-base ssDNAs with complementary sequences exhibits sufficient binding specificity for QD labeling, even when using random sequences. Further, the binding between ssDNA–DPPEs and ssDNA–QDs was sensitive to DNase treatment (Figure 2G). Specifically, 0.05% DNase treatment of neurons labeled with random1S–DPPE and random1AS–QDs reduced the number of QDs in the same field, whereas the mock group remained unchanged before and after the addition of DNase (Figures 2H, 2I, Supplementary Table S2). This further emphasizes that the QD labeling was not nonspecific but instead oligo DNA-dependent. Collectively, the hybridization of ssDNAs with complementary sequences applies to the specific labeling of membrane molecules with QDs.

Measurement of the Diffusion coefficient of DPPE by oligo DNA-dependent QD-SPT

We investigated the suitability of DPPE labeled with QDs through DNA hybridization for SPT. In some cell types, the diffusion of membrane molecules at the cell bottom, where cells contact the cover glass, is reduced compared with the cell surface [27] [28]. A TIRFM was used to measure the diffusion coefficient of the DPPE fused with the organic dye ATTO647 (ATTO647–DPPE) in the primary neurons at the surface and the bottom of the same cell [24] (Figure 3A). The diffusion coefficient (*D*) of ATTO647–DPPE at the bottom (median: 1.15×10^{-1} μm²/s) was significantly lower than that at the cell surface (median: 2.21×10^{-1} μm²/s) (Figures 3B, 3C, Supplementary Table S2), indicating the reduced lateral mobility of DPPE at the bottom of the neuron primary culture. The diffusion coefficient of polyT–DPPE labeled with polyA–QDs was measured at both the surface and the bottom of cultured neurons (Figure 3D). The trajectories of QD–polyA/polyT–DPPE complex exhibited the lateral diffusion on the plasma membrane (Figure 3E), indicating that the QD labeling through oligo DNA is stable enough to enable tracking diffusion dynamics of membrane molecules. The percentage of the immobile QDs, QDs with *D* of less than 4.00×10^{-4} μm²/s [21], was significantly larger at the cell bottom (median: 17.3%) than at the surface (median: 2.16%) (Figure 3F, Supplementary Table S2). Furthermore, the *D* of mobile QD–ssDNA–DPPE remained lower at the bottom (median: 0.82×10^{-1} μm²/s) than at the surface (median: 1.86×10^{-1} μm²/s), with a greater proportion of low diffusion coefficients at the bottom (Figures 3G, 3H, Supplementary Table 2). These results indicate that the diffusion of the QD–oligo DNA–DPPE complex is suppressed at the bottom of cultured neurons, in coordination with the result of ATTO647-conjugated DPPE whose molecular size is smaller compared with QDs (Figures 3B, 3C). However, a more immobile QD fraction and a lower *D* at the cell bottom indicate the existence of steric hindrance due to the relatively large size of QD compared with organic dyes. These findings indicate that molecules on the surface layer, where the effect of physical diffusion suppression is minimal, need to be considered for analysis in subsequent experiments measuring *D*.

Impacts of ssDNA Sequence on QD Labeling Efficacy and Diffusion Coefficient

We examined whether ssDNA sequence affects the QD binding affinity and diffusion coefficient with the ssDNA sequence pair of polyA and polyT (melting temperature [Tm] 52.17°C) and random1S/1AS (Tm: 64.47°C) (Figure 4A). The same ssDNA–DPPE (5 μg/mL) and ssDNA–QD (0.25 μM) concentration resulted in a higher number of QDs per image in the polyA/polyT ssDNA pair group than the random1S/1AS pair (Figure 4B, Supplementary Table S2). Despite having the lower Tm, polyA/polyT combination detected ~10 fold more QDs (median:193 QDs/image), compared with random1S/1AS (median: 20 QDs/image) (Figure 4C, Supplementary Table S2). This indicates that the poly ssDNA sequence has higher labeling efficacy compared with the random sequence under current experimental conditions. QD-SPT should be performed at a sufficiently low density so that each QD can be identified as a single particle optically without overlapping the trajectory [9]. Therefore, ssDNA–DPPE and ssDNA–QD concentrations were adjusted based on the oligo DNA pair sequence in experiments conducted thereafter; thus, fewer than ~50 QDs are found in one field of view (polyA/polyT pair: 1 μg/mL ssDNA–DPPE and 0.063 μM ssDNA–QD; random sequence pair: 20 μg/mL ssDNA–DPPE and 0.25 μM ssDNA–QD).

To investigate the association of ssDNA sequences with the diffusion dynamics of target molecules, we compared the diffusion dynamics of DPPE labeled with QDs conjugated to either polyA/polyT pair or random1S/1AS pair. The trajectories of QD–oligo DNA–DPPE complex of both polyA/polyT pair and random1S–AS pair exhibited similar diffusion behavior on the plasma membrane (Figure 4D). No significant difference in the median and distribution of diffusion coefficients was found between the polyA/polyT pair and the random1S/1AS pair (Figures 4E, 4F, Supplementary Table S2). These results indicate that the sequence of linker ssDNA affects labeling efficacy but has little effect on the diffusion coefficient of oligo DNA-based QD-SPT.

DNA-based QD-SPT for membrane proteins comparable to conventional QD-SPT

We further applied oligoDNA-dependent QD labeling to the diffusion analysis of a membrane protein. Here, for the proof of concept, we selected an inhibitory neurotransmitter receptor $GABA_AR$, whose diffusion behavior on the neuron has been analyzed using conventional QD-SPT [23,29-31]. PolyA ssDNA was conjugated to the anti-$GABA_AR$ antibody (polyA-Ab) and targeted to the endogenous $GABA_ARs$ in the neuronal plasma membrane, followed by the incubation with polyA–QD or polyT–QD (Figure 5A). Only polyT–QD, which are complementary to the polyA sequence, bound to polyA–$GABA_AR$ (Figure 5B). The median number of QDs per

image was 2 for polyA–QD and 28 for polyT–QD (Figure 5C, Supplementary Table S2). These results indicate that QDs can be specifically targeted to the protein of interest via oligo DNA hybridization.

We then compared oligo DNA-based QD-SPT with conventional QD-SPT, which targets QDs via secondary antibody Fab. PolyA-Abs on the $GABA_AR$ were labeled with polyT–QDs (oligo DNA) or with a conventional method using biotinylated Fab antibodies and streptavidin–QDs (Fab) (Figure 5D). In both methods, QD-labeled $GABA_ARs$ demonstrated diffusive behavior on the neuronal membrane (Figure 5E), with no statistically significant difference in the median D (Figure 5F, ssDNA: 6.49×10^{-2} μm²/s; Fab: 5.19×10^{-2} μm²/s). However, analysis of the distribution of D revealed a tendency for D-values to be high in the slow fraction of QDs–oligo DNA–$GABA_AR$ (Figure 5G; Kolmogorov–Smirnov test, $p = 0.012$, $D_{KS} = 0.080$). Collectively, oligo DNA-based labeling functions as an effective alternative method to secondary antibody Fab labeling in QD-SPT of membrane proteins. However, differences in the linkers between QD and protein may affect the distribution of D.

Multicolor imaging of the dynamics of lipids and proteins with oligo DNA-based QD-SPT

The results obtained so far demonstrate that oligo DNA-based QD-SPT can be applied to both membrane lipids and membrane proteins, yielding results equivalent to those obtained using conventional labeling methods. Finally, we verified whether the simultaneous measurement of diffusion of multiple membrane molecules within the same neurons using oligonucleotide-based QD-SPT, with QDs emitting fluorescence of different wavelengths.

$GABA_AR$ were targeted with polyA–Ab and polyT–QD605 ($GABA_AR$–QD605), and random1S–DPPE were labeled with random1AS–QD655 (DPPE–QD655) (Figure 6A). The 100-frame trajectories (~8 s) of $GABA_AR$–QD605 were shorter than those of DPPE–QD655 (Figure 6B), suggesting different diffusion dynamics. DPPE-QD655 (median: 1.15×10^{-1} μm²/s) demonstrated significantly higher D than $GABA_AR$–QD605 (median: 2.32×10^{-2} μm²/s) (Figure 6C, Supplementary Table S2), and the distributions of D were markedly different (Figure 6D; Kolmogorov–Smirnov test, $p < 0.001$, $Dks = 0.300$). The median D and interquartile range obtained using the single-wavelength QD-SPT were comparable to those obtained with multicolor QD-SPT (Table S2). This indicates that two-color QD-SPT using ssDNA enables the simultaneous targeting and discrimination of two distinct membrane molecules via different QD emission wavelengths.

Discussion

In the present study, we demonstrated a method for labeling membrane molecules with QDs using the hybridization between ssDNAs with complementary sequences. This oligo DNA-based QD labeling was stable enough for tracking the dynamics of membrane molecules and compatible with conventional QD-SPT using a secondary antibody Fab. Furthermore, using different ssDNA sequences to label multiple types of membrane proteins with QDs of various wavelengths, we established multicolor QD-SPT, which enables observation of the dynamics of multiple membrane molecules, i.e., DPPE and $GABA_ARs$, within the same cell.

QD labeling of membrane molecules via oligo DNA and dependence on the sequence

QDs exhibit a broad absorption spectrum and a narrow fluorescence spectrum, enabling excitation with a single light source and separation of multiple fluorescence signals. These QD characteristics are desirable properties for multicolor imaging, which enables the observation of different targets at various wavelengths in the same cell. Studies have labeled multiple types of molecules with QDs of different wavelengths in fixed cells [13] [14] [15]; however, most targets of QD-SPT in live cells were a single type of molecule. One of the reasons for this limitation was the combination of linkers connecting the membrane molecules and QD, such as the animal species of antibodies, and the number of protein-ligand interactions. In this study, we aimed to overcome this limitation of the number of combinations by applying hybridization between ssDNA, which generates numerous specific interactions based on the sequence. All 20 base oligo DNAs designed in this study, polyA/polyT pair, random1S/1AS pair, and random2S/2AS pairs, provided sufficient binding affinity and specificity, enabling hybridization-dependent labeling with QDs to DPPE molecules inserted in the plasma membrane. However, the number of QDs bound differed according to the sequence of linker oligo DNA. More QD bindings were observed when poly ssDNA was used as a linker, compared with random sequence. Under our experimental condition at 37°C, over 10-fold more QDs were found with polyA/polyT pair without guanine–cytosine pair than with random1S/1AS pair which has a higher Tm, although lower DNA duplex stability was expected for polyA/polyT combination (Tm: 52.17°C) compared with random1S/1AS pair (Tm: 64.47°C) [32]. One explanation for the

higher binding of QDs by polyA/polyT pair is the high degree of freedom in sequence overlap, enabling stable binding even if only part of the 20-mer hybridizes. Further, ssDNAs with a random sequence can form secondary structures through base pairing. Indeed, secondary structure prediction of random ssDNA sequences using mFold [33] indicated the formation of secondary structures, which may inhibit the access to the complementary strand (Supplementary Figure S3), resulting in fewer observed QD counts. The minimum free energy change (ΔG) for these secondary structure formations is −1.74 kcal/mol or higher. Conversely, the free energy change during hybridization of complementary strands of random sequences calculated using DINAmelt [34] was −20 kcal/mol or higher, indicating that hybridization between complementary strands is more stable compared with secondary structure within the ssDNA. The DNA hybridization time was set to 1 min in the present study; however, extending the incubation time to reach equilibrium could potentially yield different results for the observed QD counts. However, the diffusion parameters, such as D, were not affected by the ssDNA sequence under conditions where the number of QD bindings per field of view was adjusted to be suitable for SPT. These results indicate that both poly ssDNA and random ssDNA are available for oligo DNA-based QD-SPT linkers.

Pros and cons of oligo DNA-based QD-SPT against SFT

As reported in other cultured cells [27] [28], the diffusion dynamics of phospholipids vary between the surface and bottom layers of primary cultured rat hippocampal neurons. The D of DPPE labeled with ATTO647 was lower in the bottom layer than in the surface layer. Further, the D at the cell bottom obtained by oligo DNA-based QD-SPT was significantly lower than that in the surface layer, with an increased proportion of immobile QDs. Although limited to mobile QD fractions, the D of DPPE measured in the bottom layer was significantly lower than that in the surface layer. These results indicate that oligo DNA-based QD-SPT can reliably detect differences in diffusion dynamics at the subcellular level. However, only QD–oligo DNA–DPPE exhibited lower D ($< 10^{-3}$ μm²/s) and immobile fractions ($D < 0.0004$ μm²/s) in the bottom layer, which were not observed in the ATTO647–DPPE group. The size of organic dyes is approximately 1–2 nm, whereas QDs with functionalization layers are approximately 15–30 nm [35]. Therefore, interactions between the QD as a probe and glycans or the extracellular matrix may affect the lateral diffusion of cell membrane molecules. The diffusion of QD-conjugated membrane proteins, calcium-activated potassium channels and B cell receptors, is significantly reduced at the bottom layer of the cell compared with proteins labeled with organic dyes [36] [37]. The difference in diffusion motion observed in this study between ATTO647-labeled DPPE and QD-labeled DPPE at the bottom layer of the cell may indicate the existence of steric hindrance that affects phospholipid diffusion. However, noteworthily, the localization accuracy for single molecules decreases in single-fluorescence tracking due to the low number of photons [38]. DPPE with D of $< 10^{-3}$ μm²/s was not observed in the ATTO647 SFT due to the reduced localization accuracy compared to those from QDs caused by the lower number of photons from single fluorophores. The main advantages of QDs are their bright fluorescence, which provides a high SNR, and their long fluorescence lifetime, which enables stable tracking. QD-SPT is a practical choice in environments where small spatial obstacles are expected, and when high localization accuracy and long trajectories are required.

Effect of linkers on the protein diffusion measured by QD-SPT

We used the $GABA_AR$ for the example of the membrane proteins to compare oligo DNA-based QD-SPT with the widely used conventional QD-SPT using Fab fragments. The QD labeling achieved through ssDNA hybridization also maintained sufficient specificity and stability for SPT, such as labeling using the interaction between primary and secondary antibodies. The D of $GABA_AR$ showed no significant difference in their median values between the oligo DNA-based QD-SPT and the conventional QD-SPT. However, in the oligo DNA-QD-SPT method, the proportion of QDs showed significantly higher D in the fraction with low diffusion coefficients (K–S test, $P = 0.012$) compared with QD conjugated through Fab. The impact on the overall distribution of D was small (K–S test D_{KS} value = 0.080); however, the potential influence of the linker between QDs and target molecules should be fully considered when combining the DNA method and the antibody approach for membrane proteins.

The labeling using annealing between complementary ssDNA strands is an effective method for increasing the number of specific intermolecular bonds; however, the process of fusing oligoDNAs to primary antibodies has been a major challenge. Advancements in copper-free click chemistry, which was utilized for the DPPE label in this study, have profoundly transformed the landscape of the field of bioconjugation. The increased availability of modified oligoDNAs and reagents for click chemistry enabled the fusion of oligonucleotides to antibodies and

biomolecules in a few steps at room temperature via chemical reactions in biological laboratories [19]. Therefore, protein labeling using oligonucleotides as linkers is expected to be an option in the future.

The hydrodynamic radius of the Fab antibody is approximately 2.5 nm [39], and the hydrodynamic radius of the 20-base double-strand DNA is estimated to be 4–6 nm [40], indicating the comparability of the overall size of the Fab-QD and DNA-QD probes. The root mean square deviation calculated by molecular dynamics simulations is of the same order (1–5 Å), [41] [42] [43] [44], suggesting that differences in the size or rigidity of the linker molecules cannot explain the difference in diffusion dynamics. The mechanism by which differences in the linker result in variations in the diffusion coefficient remains to be clarified in future studies.

Prospects for Multicolor QD-SPT

QDs with sharp fluorescent spectra are ideal probes for multicolor imaging. Labeling the same membrane molecules with QDs of eight wavelengths helps avoid trajectory overlap in the same field of view, enabling tracking of the dynamics of more QDs, thereby significantly increasing the throughput of QD-SPT [45]. In this study, we aimed to develop a new labeling method that utilizes the sequence specificity of ssDNA hybridization to target QDs of different wavelengths to specific targets. We successfully fused QD655 and QD605 to different targets, namely lipids (DPPE) and membrane proteins ($GABA_AR$), respectively. The biotin–streptavidin interaction used for linking QD and oligoDNA forms a firm non-covalent bond (dissociation constant Kd $=10^{-15}$ M) [46], and the possibility of dissociation is expected to be extremely low. The biotin–streptavidin binding was sufficiently stable not to allow cross-talk between QDs, considering the finding that DPPE and $GABA_AR$ diffusion, both of which have significantly different diffusion coefficients, could be distinguished using QD655 and QD605.

Here, we performed a two-color QD-SPT as a proof of concept for the availability of oligo DNA for live-cell multicolor imaging. Previous studies using fixed cells or fixed tissues have reported the application of QDs to multicolor detection methods. Flow cytometry was performed using simultaneous detection of 17 fluorescent probes, utilizing seven QDs and ten organic dyes [47]. Further, in single-cell imaging, a study revealed the staining of human prostate cancer cells using five types of biomolecules with five different QDs (QD525, QD565, QD605, QD655, and QD705) [48] [49]. This method requires dividing the labeling process into multiple steps and repeating the blocking of the antigenic sites of the primary antibody with a secondary antibody at saturation levels as many times as required. This approach is not ideal for SPT of live cells, which involves labeling to be performed quickly and at low density. In contrast, oligo DNA-based QD-SPT uses oligo DNA as linkers, which generates several combinations due to their sequence diversity, thereby enabling simultaneous labeling of multiple target molecules with different-colored QDs in a short time (several minutes). In principle, multicolor QD-SPT with three or more colors in the same cell is considered feasible; however, experimental verification remains a future challenge.

To perform multicolor QD-SPT, the optical system needs to be optimized using the sharp spectrum of QDs. In this study, the same field of view was recorded separately at each wavelength. Still, an optical system that simultaneously records multiple colors of QDs is desirable to be developed to minimize observation time. An image-splitting optical system can be employed to split the emission into two wavelengths and focus them onto a single camera, thereby enabling simultaneous imaging of two colors [50]. Furthermore, using two cameras and an image-splitting optical system, four colors of QDs within the same field of view is possible to be simultaneously imaged.

Conclusion

In this study, we revealed that a linker using hybridization between complementary ssDNA can be utilized for the analysis of membrane molecular dynamics with QD-SPT. The DNA-based QD labeling method developed in this study is expected to help target multiple types of molecules with different wavelength QDs in an oligo DNA sequence-specific manner. It is considered to significantly enable simultaneous multicolor QD-SPT of living cell membrane molecules.

Conflict of interest

The authors declare no conflict of interest related to this publication.

Author contributions

SS, TK, NK, TU, ME, RK, HY, HB conducted the experiment. SS, TK, NK, TU, ME, RK, CO, IK, and AC performed the analysis. YT synthesized the ssDNA–DPPE. HB designed the study and supervision of this work. All authors discussed the results and commented on the manuscript.

Data availability

The evidence data generated and/or analyzed during the current study are available from the corresponding author upon reasonable request.

Acknowledgments

The authors thank Dr. Hiromu Kashida (Nagoya University) for designing the random oligo DNA sequences, Prof. Akihiro Kusumi (OIST) for advice on single-fluorophore imaging of DPPE, Prof. Hiroaki Tateno for advice on nucleotide conjugation to antibodies, and Dr. Atushi Okazawa (Waseda University) for the support of figure preparation. This research was supported by grants from JST PRESTO JPMJPR15F8, JSPS Grants-in-Aid for Scientific Research (23K08410 to SS; 23K18116 and 23K21299 to HB), and grants from Naito Foundation and Takeda Science Foundation to HB. DeepL, ChatGPT 4o, Grammarly, and Enago, the editing brand of Crimson Interactive Pvt. Ltd supported the English editing of this article.

References

[1] Singer, S.J., Nicolson, G.L. The fluid mosaic model of the structure of cell membranes. Science 175, 720-731 (1972). https://doi.org/10.1126/science.175.4023.720

[2] Fujiwara, T., Ritchie, K., Murakoshi, H., Jacobson, K., Kusumi, A. Phospholipids undergo hop diffusion in compartmentalized cell membrane. J Cell Biol 157, 1071-1081 (2002). https://doi.org/10.1083/jcb.200202050

[3] Fujiwara, T.K., Tsunoyama, T.A., Takeuchi, S., Kalay, Z., Nagai, Y., Kalkbrenner, T., et al. Ultrafast single-molecule imaging reveals focal adhesion nano-architecture and molecular dynamics. J Cell Biol 222 (2023). https://doi.org/10.1083/jcb.202110162

[4] Poveda, J.A., Fernandez, A.M., Encinar, J.A., Gonzalez-Ros, J.M. Protein-promoted membrane domains. Biochim Biophys Acta 1778, 1583-1590 (2008). https://doi.org/10.1016/j.bbamem.2008.01.021

[5] Choquet, D., Triller, A. The dynamic synapse. Neuron 80, 691-703 (2013). https://doi.org/10.1016/j.neuron.2013.10.013

[6] Nakada, C., Ritchie, K., Oba, Y., Nakamura, M., Hotta, Y., Iino, R., et al. Accumulation of anchored proteins forms membrane diffusion barriers during neuronal polarization. Nat Cell Biol 5, 626-632 (2003). https://doi.org/10.1038/ncb1009

[7] Alcor, D., Gouzer, G., Triller, A. Single-particle tracking methods for the study of membrane receptors dynamics. Eur J Neurosci 30, 987-997 (2009). https://doi.org/10.1111/j.1460-9568.2009.06927.x

[8] Resch-Genger, U., Grabolle, M., Cavaliere-Jaricot, S., Nitschke, R., Nann, T. Quantum dots versus organic dyes as fluorescent labels. Nat Methods 5, 763-775 (2008). https://doi.org/10.1038/nmeth.1248

[9] Groc, L., Lafourcade, M., Heine, M., Renner, M., Racine, V., Sibarita, J.B., et al. Surface trafficking of neurotransmitter receptor: Comparison between single-molecule/quantum dot strategies. J Neurosci 27, 12433-12437 (2007). https://doi.org/10.1523/jneurosci.3349-07.2007

[10] Cai, E., Ge, P., Lee, S.H., Jeyifous, O., Wang, Y., Liu, Y., et al. Stable small quantum dots for synaptic receptor tracking on live neurons. Angew Chem Int Ed Engl 53, 12484-12488 (2014). https://doi.org/10.1002/anie.201405735

[11] Ha, T., Tinnefeld, P. Photophysics of fluorescent probes for single-molecule biophysics and super-resolution imaging. Annu Rev Phys Chem 63, 595-617 (2012). https://doi.org/10.1146/annurev-physchem-032210-103340

[12] Medintz, I.L., Uyeda, H.T., Goldman, E.R., Mattoussi, H. Quantum dot bioconjugates for imaging, labelling and sensing. Nat Mater 4, 435-446 (2005). https://doi.org/10.1038/nmat1390

[13] Arnspang, E.C., Brewer, J.R., Lagerholm, B.C. Multi-color single particle tracking with quantum dots. PLoS One 7, e48521 (2012). https://doi.org/10.1371/journal.pone.0048521

[14] Zrazhevskiy, P., Gao, X. Quantum dot imaging platform for single-cell molecular profiling. Nature Communications 4, 1619 (2013). https://doi.org/10.1038/ncomms2635

[15] Wang, W., Liu, Z., Lan, X. Quantum dot-based simultaneous multicolor imaging. Mol Imaging Biol 22, 820-831 (2020). https://doi.org/10.1007/s11307-019-01432-4

[16] Jungmann, R., Avendano, M.S., Woehrstein, J.B., Dai, M., Shih, W.M., Yin, P. Multiplexed 3d cellular super-resolution imaging with DNA-paint and exchange-paint. Nat Methods 11, 313-318 (2014). https://doi.org/10.1038/nmeth.2835
[17] Bannai, H., Hirose, M., Niwa, F., Mikoshiba, K. Dissection of local ca2+ signals in cultured cells by membrane-targeted ca2+ indicators. J Vis Exp (2019). https://doi.org/10.3791/59246
[18] Teramura, Y. Cell surface modification with ssdna-peg-lipid for analysing intercellular interactions between different cells. Biomaterials 48, 119-128 (2015). https://doi.org/10.1016/j.biomaterials.2015.01.032
[19] Maerle, A.V., Simonova, M.A., Pivovarov, V.D., Voronina, D.V., Drobyazina, P.E., Trofimov, D.Y., et al. Development of the covalent antibody-DNA conjugates technology for detection of ige and igm antibodies by immuno-pcr. PLoS One 14, e0209860 (2019). https://doi.org/10.1371/journal.pone.0209860
[20] Sun, N., Tran, B.V., Peng, Z., Wang, J., Zhang, C., Yang, P., et al. Coupling lipid labeling and click chemistry enables isolation of extracellular vesicles for noninvasive detection of oncogenic gene alterations. Adv Sci (Weinh) 9, e2105853 (2022). https://doi.org/10.1002/advs.202105853
[21] Bannai, H., Inoue, T., Hirose, M., Niwa, F., Mikoshiba, K. Synaptic function and neuropathological disease revealed by quantum dot-single-particle tracking. in Single molecule microscopy in neurobiology. (Yamamoto, N., Okada, Y. eds.), pp. 131-155 Springer US, New York, NY (2020).
[22] Niwa, F., Bannai, H., Arizono, M., Fukatsu, K., Triller, A., Mikoshiba, K. Gephyrin-independent gaba(a)r mobility and clustering during plasticity. PLoS One 7, e36148 (2012). https://doi.org/10.1371/journal.pone.0036148
[23] Bannai, H., Niwa, F., Sherwood, M.W., Shrivastava, A.N., Arizono, M., Miyamoto, A., et al. Bidirectional control of synaptic gabaar clustering by glutamate and calcium. Cell Rep 13, 2768-2780 (2015). https://doi.org/10.1016/j.celrep.2015.12.002
[24] Nishiguchi, T., Yoshimura, H., Kasai, R.S., Fujiwara, T.K., Ozawa, T. Synergetic roles of formyl peptide receptor 1 oligomerization in ligand-induced signal transduction. ACS Chem Biol 15, 2577-2587 (2020). https://doi.org/10.1021/acschembio.0c00631
[25] Inoue, T., TI Workbench, an integrated software package for electrophysiology and imaging. Microscopy 67(3), 129-143 (2018). https://doi.org/10.1093/jmicro/dfy015.
[26] Saxton, M. J., Jacobson, K. Single-particle tracking: applications to membrane dynamics. Annual review of biophysics and biomolecular structure 26, 373–399 (1997). https://doi.org/10.1146/annurev.biophys.26.1.373
[27] Tournier, J.F., Lopez, A., Tocanne, J.F. Effect of cell substratum on lateral mobility of lipids in the plasma membrane of vascular endothelial cells. Exp Cell Res 181, 105-115 (1989). https://doi.org/10.1016/0014-4827(89)90186-9
[28] Makaremi, S., Rose, M., Ranjit, S., Digman, M.A., Bowdish, D.M.E., Moran-Mirabal, J.M. Lateral diffusion of cd14 and tlr2 in macrophage plasma membrane assessed by raster image correlation spectroscopy and single particle tracking. Scientific Reports 10, 19375 (2020). https://doi.org/10.1038/s41598-020-76272-2
[29] Muir, J., Arancibia-Carcamo, I.L., MacAskill, A.F., Smith, K.R., Griffin, L.D., Kittler, J.T. Nmda receptors regulate gabaa receptor lateral mobility and clustering at inhibitory synapses through serine 327 on the γ2 subunit. Proc Natl Acad Sci U S A 107, 16679-16684 (2010). https://doi.org/10.1073/pnas.1000589107
[30] Merlaud, Z., Marques, X., Russeau, M., Saade, U., Tostain, M., Moutkine, I., et al. Conformational state-dependent regulation of gaba(a) receptor diffusion and subsynaptic domains. iScience 25, 105467 (2022). https://doi.org/10.1016/j.isci.2022.105467
[31] Battaglia, S., Renner, M., Russeau, M., Côme, E., Tyagarajan, S.K., Lévi, S. Activity-dependent inhibitory synapse scaling is determined by gephyrin phosphorylation and subsequent regulation of gaba_a receptor diffusion. eneuro 5, ENEURO.0203-0217.2017 (2018). https://doi.org/10.1523/eneuro.0203-17.2017
[32] Breslauer, K.J., Frank, R., Blocker, H., Marky, L.A. Predicting DNA duplex stability from the base sequence. Proc Natl Acad Sci U S A 83, 3746-3750 (1986). https://doi.org/10.1073/pnas.83.11.3746
[33] Zuker, M. Mfold web server for nucleic acid folding and hybridization prediction. Nucleic Acids Res 31, 3406-3415 (2003). https://doi.org/10.1093/nar/gkg595
[34] Markham, N.R., Zuker, M. Dinamelt web server for nucleic acid melting prediction. Nucleic Acids Res 33, W577-581 (2005). https://doi.org/10.1093/nar/gki591
[35] Manzo, C., Garcia-Parajo, M.F. A review of progress in single particle tracking: From methods to biophysical insights. Rep Prog Phys 78, 124601 (2015). https://doi.org/10.1088/0034-4885/78/12/124601
[36] Nechyporuk-Zloy, V., Dieterich, P., Oberleithner, H., Stock, C., Schwab, A. Dynamics of single potassium channel proteins in the plasma membrane of migrating cells. Am J Physiol Cell Physiol 294, C1096-1102 (2008). https://doi.org/10.1152/ajpcell.00252.2007
[37] Abraham, L., Lu, H.Y., Falcão, R.C., Scurll, J., Jou, T., Irwin, B., et al. Limitations of qdot labelling compared to directly-conjugated probes for single particle tracking of b cell receptor mobility. Scientific Reports 7,

11379 (2017). https://doi.org/10.1038/s41598-017-11563-9
[38] Ober, R.J., Ram, S., Ward, E.S. Localization accuracy in single-molecule microscopy. Biophys J 86, 1185-1200 (2004). https://doi.org/10.1016/s0006-3495(04)74193-4
[39] Shatz, W., Hass, P.E., Mathieu, M., Kim, H.S., Leach, K., Zhou, M., et al. Contribution of antibody hydrodynamic size to vitreal clearance revealed through rabbit studies using a species-matched fab. Mol Pharm 13, 2996-3003 (2016). https://doi.org/10.1021/acs.molpharmaceut.6b00345
[40] Fernandes, M.X., Ortega, A., López Martínez, M.C., García de la Torre, J. Calculation of hydrodynamic properties of small nucleic acids from their atomic structure. Nucleic Acids Res 30, 1782-1788 (2002). https://doi.org/10.1093/nar/30.8.1782
[41] Young, M.A., Ravishanker, G., Beveridge, D.L. A 5-nanosecond molecular dynamics trajectory for b-DNA: Analysis of structure, motions, and solvation. Biophys J 73, 2313-2336 (1997). https://doi.org/10.1016/s0006-3495(97)78263-8
[42] Dixit, S.B., Ponomarev, S.Y., Beveridge, D.L. Root mean square deviation probability analysis of molecular dynamics trajectories on DNA. J Chem Inf Model 46, 1084-1093 (2006). https://doi.org/10.1021/ci0504925
[43] Li, T., Tracka, M.B., Uddin, S., Casas-Finet, J., Jacobs, D.J., Livesay, D.R. Rigidity emerges during antibody evolution in three distinct antibody systems: Evidence from qsfr analysis of fab fragments. PLoS Comput Biol 11, e1004327 (2015). https://doi.org/10.1371/journal.pcbi.1004327
[44] Tang, J., Zhang, C., Castillo, N.C., Lalaurie, C.J., Gao, X., Dalby, P.A., et al. Crystal structures and molecular dynamics simulations of a humanised antibody fragment at acidic to basic ph. Scientific Reports 13, 16281 (2023). https://doi.org/10.1038/s41598-023-42698-7
[45] Cutler, P.J., Malik, M.D., Liu, S., Byars, J.M., Lidke, D.S., Lidke, K.A. Multi-color quantum dot tracking using a high-speed hyperspectral line-scanning microscope. PLoS One 8, e64320 (2013). https://doi.org/10.1371/journal.pone.0064320
[46] Green, N.M. Avidin. in Advances in protein chemistry. (Anfinsen, C.B., Edsall, J.T., Richards, F.M. eds.) vol. 29, pp. 85-133 Academic Press, (1975).
[47] Chattopadhyay, P.K., Perfetto, S.P., Yu, J., Roederer, M. The use of quantum dot nanocrystals in multicolor flow cytometry. Wiley Interdiscip Rev Nanomed Nanobiotechnol 2, 334-348 (2010). https://doi.org/10.1002/wnan.75
[48] Xing, Y., Smith, A.M., Agrawal, A., Ruan, G., Nie, S. Molecular profiling of single cancer cells and clinical tissue specimens with semiconductor quantum dots. Int J Nanomedicine 1, 473-481 (2006). https://doi.org/10.2147/nano.2006.1.4.473
[49] Xing, Y., Chaudry, Q., Shen, C., Kong, K.Y., Zhau, H.E., Chung, L.W., et al. Bioconjugated quantum dots for multiplexed and quantitative immunohistochemistry. Nat Protoc 2, 1152-1165 (2007). https://doi.org/10.1038/nprot.2007.107
[50] Juette, M.F., Terry, D.S., Wasserman, M.R., Zhou, Z., Altman, R.B., Zheng, Q., et al. The bright future of single-molecule fluorescence imaging. Curr Opin Chem Biol 20, 103-111 (2014). https://doi.org/10.1016/j.cbpa.2014.05.010

Figure Legends

Figure 1. Overview of the ssDNA labeling protocol used in this experiment
DPPE conjugated with a 20-mer ssDNA (ssDNA–DPPE), or an anti-$GABA_AR$ antibody conjugated with DNA (ssDNA–Ab), and QDs modified with ssDNA via streptavidin–biotin interaction (ssDNA–QD) were prepared. Primary rat hippocampal neurons were incubated with ssDNA–DPPE or ssDNA–Ab for 5 min, followed by a 1-min incubation with ssDNA–QD, in a humid chamber maintained at 37°C.

Figure 2. QD labeling of membrane lipids via complementary DNA sequences
(A) Schematic illustration of QD labeling of DPPE via complementary DNA sequences. PolyA–DPPE was incorporated into the plasma membrane of primary culture neurons and subsequently incubated with polyA–QDs or polyT–QDs. (B) Representative QD images after labeling polyA–DPPE with polyA–QDs (left) or polyT–QDs (right). Scale bar indicates 10 µm. (C) Number of polyA–QDs and polyT–QDs per image on the cell surface bound to polyA–DPPE. N =10 images for both groups. The solid lines on the plot indicate the median. (D) Specificity test for QD labeling using random ssDNA sequences. Random1S–DPPE was labeled with one of the following probes: polyA–QD, polyT–QD, random1AS–QD (complementary to random1S), or random2AS–QD. (E) Representative QD images of random1S–DPPE labeled with DNA–QDs carrying four different ssDNA

sequences. Scale bar indicates 10 µm. (F) Number of QDs per field of view. N =10 images for all groups. Solid lines on the plot indicate the median. (G) Time course of DNase treatment. Images were acquired just before and 3 min after adding 0.05% DNase or HBSS (mock). (H) Representative QD images of the same field before and 3 min after treatment in the mock and DNase groups. Scale bar indicates 10 µm. (I) Number of QDs per field of view. N =11 images for both groups. Scale bar indicates 10 µm. Mann–Whitney U-test for (C), one-way analysis of variance with post-hoc Tukey HSD test for (F), and Wilcoxon signed-rank test for (I).

Figure 3. Diffusion dynamics of the DPPE measured using single-fluorophore imaging and oligo DNA-based QD-SPT
(A) Schematic diagram of ATTO647–DPPE labeling and the focal planes at the bottom and the surface of cultured neurons, and a typical ATTO647 fluorescence image of the surface layer. Scale bar indicates 5 µm. (B) Dot plot of the *D* of ATTO647–DPPE. (C) Cumulative plots of *D*. (D) Schematic diagram illustrating the QD labeling with polyT–DPPE and polyA–QD with the location of the imaging, and a representative fluorescent image of QDs on the cell surface. Scale bar indicates 5 µm. (E) Trajectories of QDs taken with the bottom (left) and surface (right) focused: scale bars indicate 1 µm and 0.2 µm for the inset. (F) Dot plot showing the ratio of immobile QDs per the field of view. N = (G) (H) The dot plot (G) and the cumulative plot for Mobile QDs (H). (B)(F)(G) Mann–Whitney U-test. Solid lines on the plots indicate the median. (C)(H) Kolmogorov–Smirnov test. D_{ks} indicates the Kolmogorov–Smirnov distance. N = 368 (bottom) and 584 (surface) spots for (B) and (C), N = 28 (both groups) images, N = 879 (bottom) and 815 (surface) QDs for (G) and (H).

Figure 4. Impact of oligo DNA sequence on the diffusion dynamics of QD–oligo DNA–DPPE
(A) QD labeling via complementary sequences of polyA/polyT or random ssDNA. (B) Fluorescence images of neuron surface labeled with 0.25 µM polyT–QD and 5 µg/mL of polyA–DPPE (top) or 0.25 µM random1AS–QD and 5 µg/mL of random1S–DPPE (bottom). Scale bar indicates 10 µm. (C) Number of QDs per field of view. The line indicates the median. N = 5 images for both groups. (D) Example of trajectories of QD labeled via polyA/polyT (top) or random ssDNA (bottom). Scale bar indicates 1 µm. (E, F) The dot plot (E) and cumulative probability distribution (F) of QDs labeled with polyA/polyT or random sequence oligo DNA. Solid lines on the plot indicate medians; N = 220 (poly) and 257 (random) QDs. Mann–Whitney U-test for (C and E) and Kolmogorov–Smirnov test for (F).

Figure 5. Analysis of membrane proteins with oligo DNA-based QD-SPT and conventional QD-SPT
(A) Labeling of QD with antibodies against $GABA_AR$ γ2 subunit conjugated with polyA ssDNA (polyA–Ab). PolyT–QD and polyA–QD were targeted to the polyA–Ab. (B) Representative QD images on neurons with polyA–Ab, after incubating with polyA–QD (top) or polyT–QD (bottom). Scale bar indicates 10 µm. (C) Number of QDs per field of view. Solid lines indicate the median. n = 30 images for both groups. (D) Schematic diagram of $GABA_AR$ QD labeling with oligo DNA-based labeling (oligo DNA) and conventional labeling with secondary antibody Fab fragments (Fab). (E) QD trajectories for oligo DNA-based labeling (left) and the conventional labeling (right). Scale bar indicates 1 µm. (F, G) Dot plot with the median solid lines (E) and cumulative probability distribution (F) of oligo-DNA-based or conventional DNA labeling. N = 969 (oligo DNA) and 686 (Fab). Mann–Whitney U-test for (C and F) and Kolmogorov–Smirnov test (G).

Figure 6. DNA-mediated two-color QD-SPT of $GABA_A$ receptors and DPPE
(A) Strategy of the multicolor-QD labeling of $GABA_AR$ with QD605 and DPPE with QD655, using oligoDNAs. (B) Trajectories of QD605–$GABA_AR$ (left) and QD655–DPPE (right). Scale bars indicate 1 µm. (C, D) Distinct distribution of *D* of QD605–$GABA_AR$ and QD655–DPPE, revealed by a dot plot with median (solid lines) (C) and a cumulative plot (D), N = 419 (QD605–$GABA_AR$) and 412 (QD655–DPPE). Mann–Whitney U-test for (C) and Kolmogorov–Smirnov test for (D).

ssDNA name	Sequence	Tm (ºC)
polyA	5'-AAAAAAAAAAAAAAAAAAAA-3'	52.17
polyT	5'-TTTTTTTTTTTTTTTTTTTT-3'	52.17
Random1S	5'-ATGAGGTCGTAAGCGTTCCA-3'	64.47
Random1AS	5'-TGGAACGCTTACGACCTCAT-3'	64.47
Random2S	5'-GCTACCTATGCCGTCAATGG-3'	64.21
Random2AS	5'-CCATTGACGGCATAGGTAGC-3'	64.21

Table S1 ssDNA nucleotide sequences.
List of ssDNA sequences used and melting temperatures (Tm) estimated by nearest neighbor base pairing (Breslauer et al., 1986). PolyT and PolyA, random1S and 1AS, random2S and 2AS, are complementary pairs.

Figure	group	Median (spots/image)	IQR (25% – 75%) (spots/image)	N(images)
Figure 2C	polyA-QD	1	0 – 2	10
	polyT-QD	241	96 – 400	10
Figure 2F	polyA	3	2 – 4	10
	polyT	3	2 – 4	10
	random1AS	40	26 – 49	10
	random2AS	1	0 – 2	10
Figure 2I	mock (0min)	25	17 – 29	11
	mock (3min)	27	20 – 30	
	DNase (0min)	31	24 – 33	11
	DNase (3min)	10	4 – 11	
Figure 4C	polyA-polyT	193	169 – 206	5
	random1S-1AS	20	17 – 25	5
Figure 5C	polyA-QD	2	1 – 3	30
	polyT-QD	28	22 – 44	30
Figure S1D	polyA-QD	1	0 – 1	29
	polyT-QD	22	15 – 26	30
Figure S2B	polyT-DPPE + polyA-QD	23	20 – 24	6
	polyA-QD	0	0 – 0	6
Figure S2D	random1AS	1	1 – 3	10
	random2AS	1	0 – 3	10

Figure	group	Median (μm²/s)	IQR (25% – 75%) (μm²/s)	N (QDs)
Figure 3B	bottom	1.15×10^{-1}	$5.70 – 26.6 \times 10^{-2}$	368
	surface	2.21×10^{-1}	$1.25 – 3.43 \times 10^{-1}$	584
Figure 3G	bottom	8.23×10^{-2}	$0.387 – 20.6 \times 10^{-2}$	879
	surface	1.86×10^{-1}	$9.13 – 31.5 \times 10^{-2}$	815
Figure 4E	polyA-polyT	1.38×10^{-1}	$7.74 – 22.6 \times 10^{-2}$	219
	random1S-1AS	1.47×10^{-1}	$7.86 – 23.0 \times 10^{-2}$	253
Figure 5F	ssDNA	6.49×10^{-2}	$1.41 – 12.3 \times 10^{-2}$	969
	Fab	5.19×10^{-2}	$0.841 – 12.8 \times 10^{-2}$	686
Figure 6C	$GABA_AR$	2.32×10^{-2}	$0.3 – 9.56 \times 10^{-2}$	419
	DPPE	1.15×10^{-1}	$0.826 – 24.5 \times 10^{-2}$	412

Figure	group	Median (%)	IQR (25% – 75%) (%)	N (images)
Figure 3F	bottom	17.3	4.53 – 25.1	28
	surface	2.16	0 – 7.80	28

Table S2: Summary of the median and Interquartile Range (IQR) for the data

The median and IQR of each data sets are shown here.

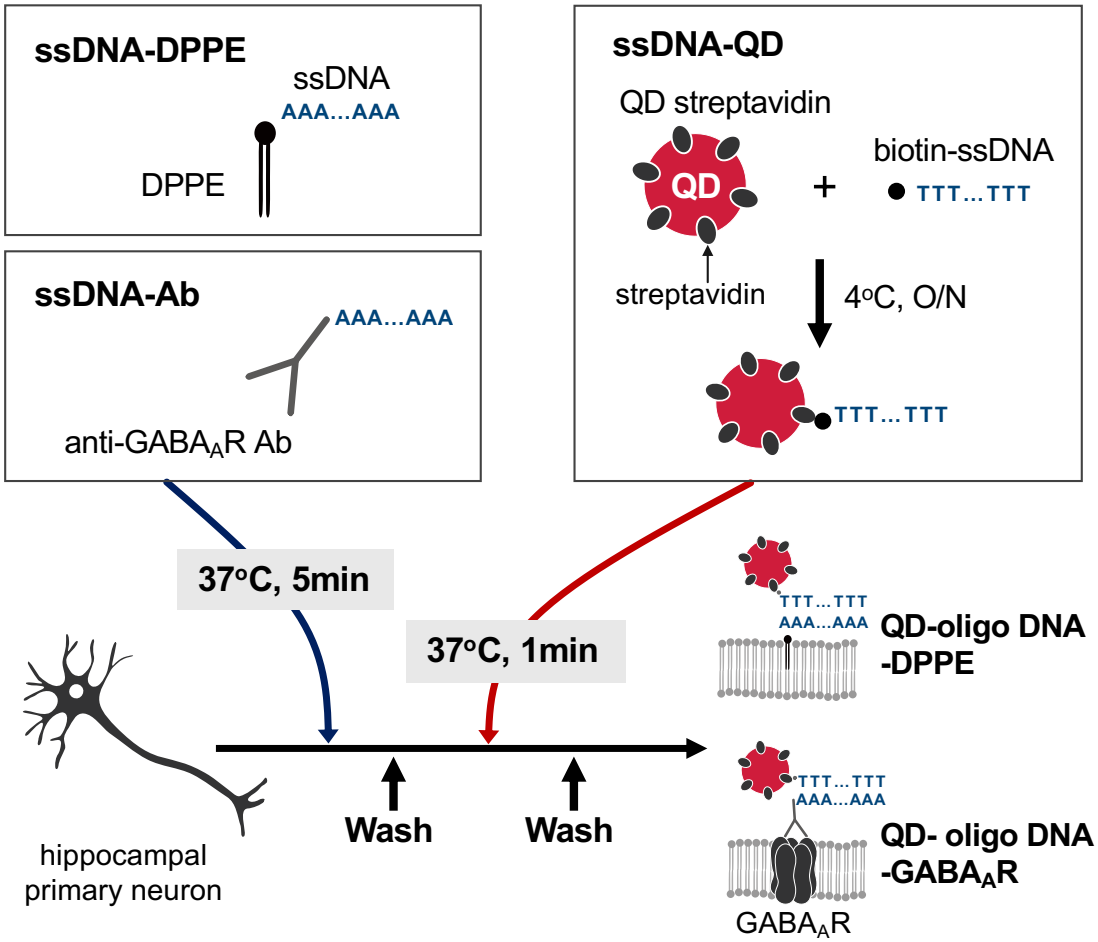
ssDNA-DPPE
ssDNA
AAA...AAA
DPPE
ssDNA-Ab
AAA...AAA
anti-GABA$_A$R Ab
ssDNA-QD
QD streptavidin
QD
+
biotin-ssDNA
TTT...TTT
streptavidin
4°C, O/N
TTT...TTT
37°C, 5min
37°C, 1min
TTT...TTT
AAA...AAA
QD-oligo DNA
-DPPE
hippocampal
primary neuron
Wash
Wash
TTT...TTT
AAA...AAA
QD- oligo DNA
-GABA$_A$R
GABA$_A$R

Figure 1

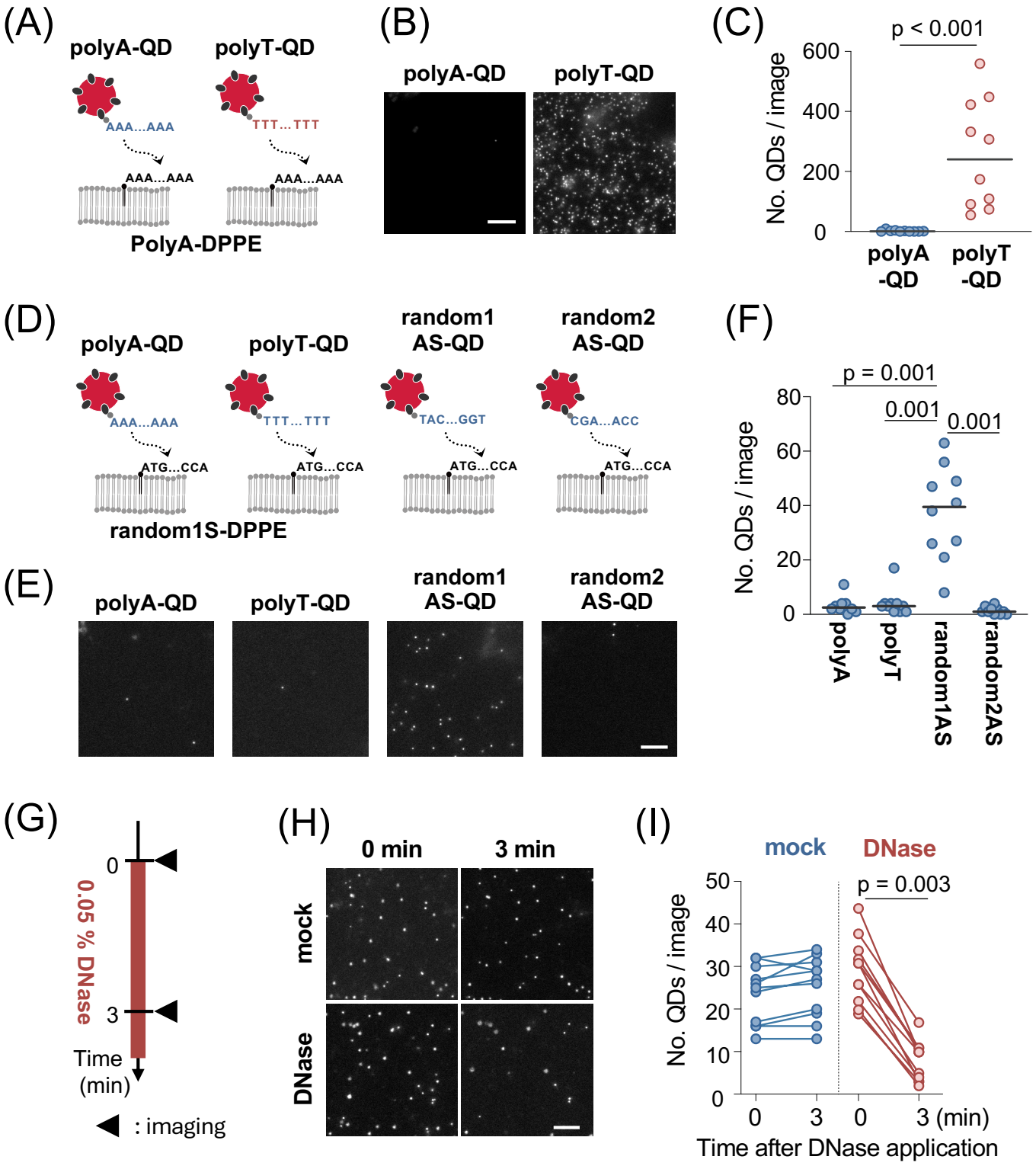
(A)
polyA-QD
polyT-QD
AAA...AAA
TTT...TTT
AAA...AAA
AAA...AAA
PolyA-DPPE
(B)
polyA-QD
polyT-QD
(C)
p < 0.001
No. QDs / image
600
400
200
0
polyA -QD
polyT -QD
(D)
polyA-QD
polyT-QD
random1 AS-QD
random2 AS-QD
AAA...AAA
TTT...TTT
TAC...GGT
CGA...ACC
ATG...CCA
ATG...CCA
ATG...CCA
ATG...CCA
random1S-DPPE
(E)
polyA-QD
polyT-QD
random1 AS-QD
random2 AS-QD
(F)
p = 0.001
0.001
0.001
No. QDs / image
80
60
40
20
0
polyA
polyT
random1AS
random2AS
(G)
0
3
0.05 % DNase
Time (min)
: imaging
(H)
0 min
3 min
mock
DNase
(I)
mock
DNase
p = 0.003
No. QDs / image
50
40
30
20
10
0
0
3
0
3 (min)
Time after DNase application

Figure 2

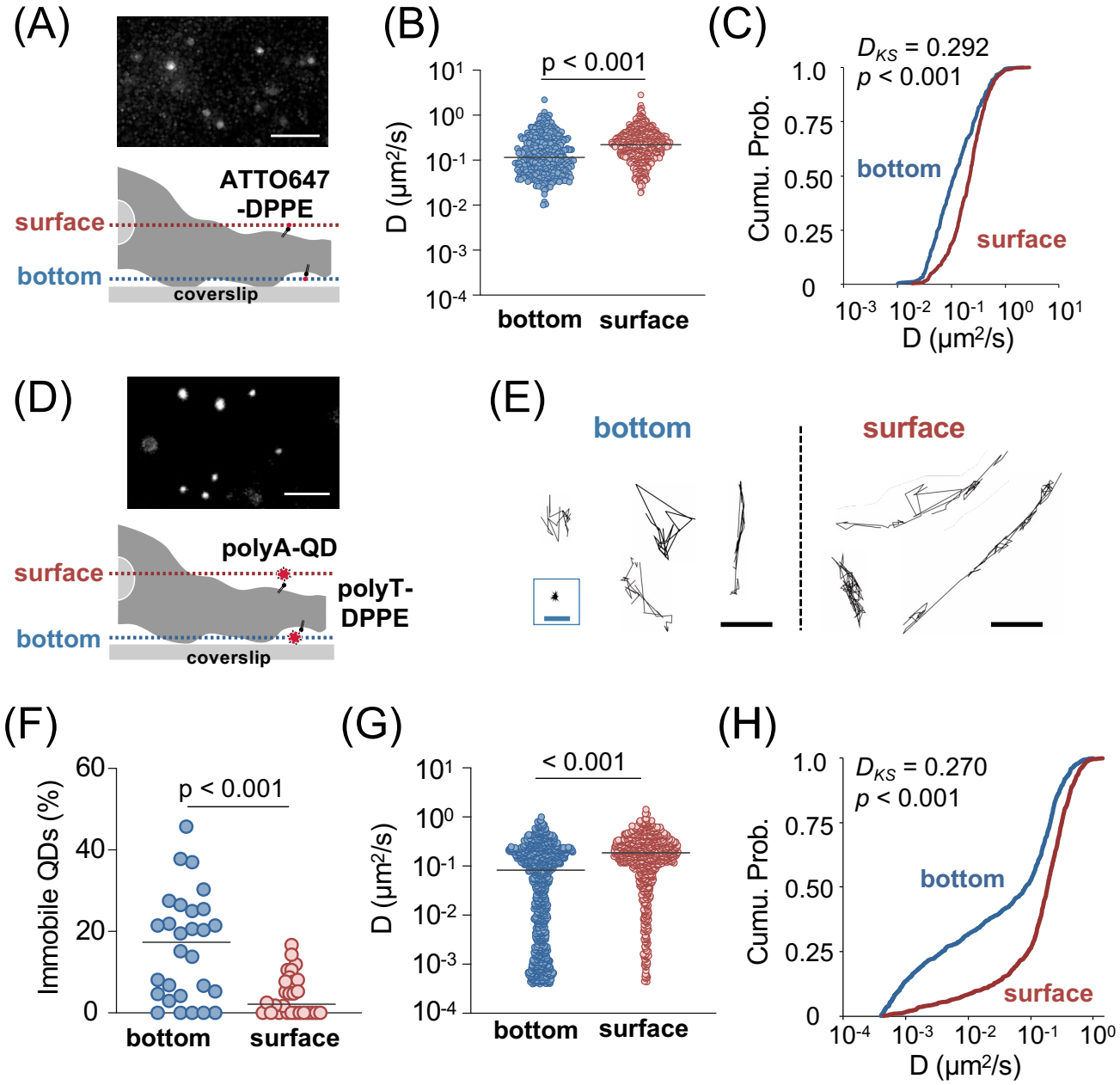
(A)
ATTO647
-DPPE
surface
bottom
coverslip
(B)
p < 0.001
D (μm²/s)
bottom
surface
(C)
D_{KS} = 0.292
p < 0.001
Cumu. Prob.
bottom
surface
D (μm²/s)
(D)
polyA-QD
polyT-
DPPE
surface
bottom
coverslip
(E)
bottom
surface
(F)
p < 0.001
Immobile QDs (%)
bottom
surface
(G)
< 0.001
D (μm²/s)
bottom
surface
(H)
D_{KS} = 0.270
p < 0.001
Cumu. Prob.
bottom
surface
D (μm²/s)

Figure 3

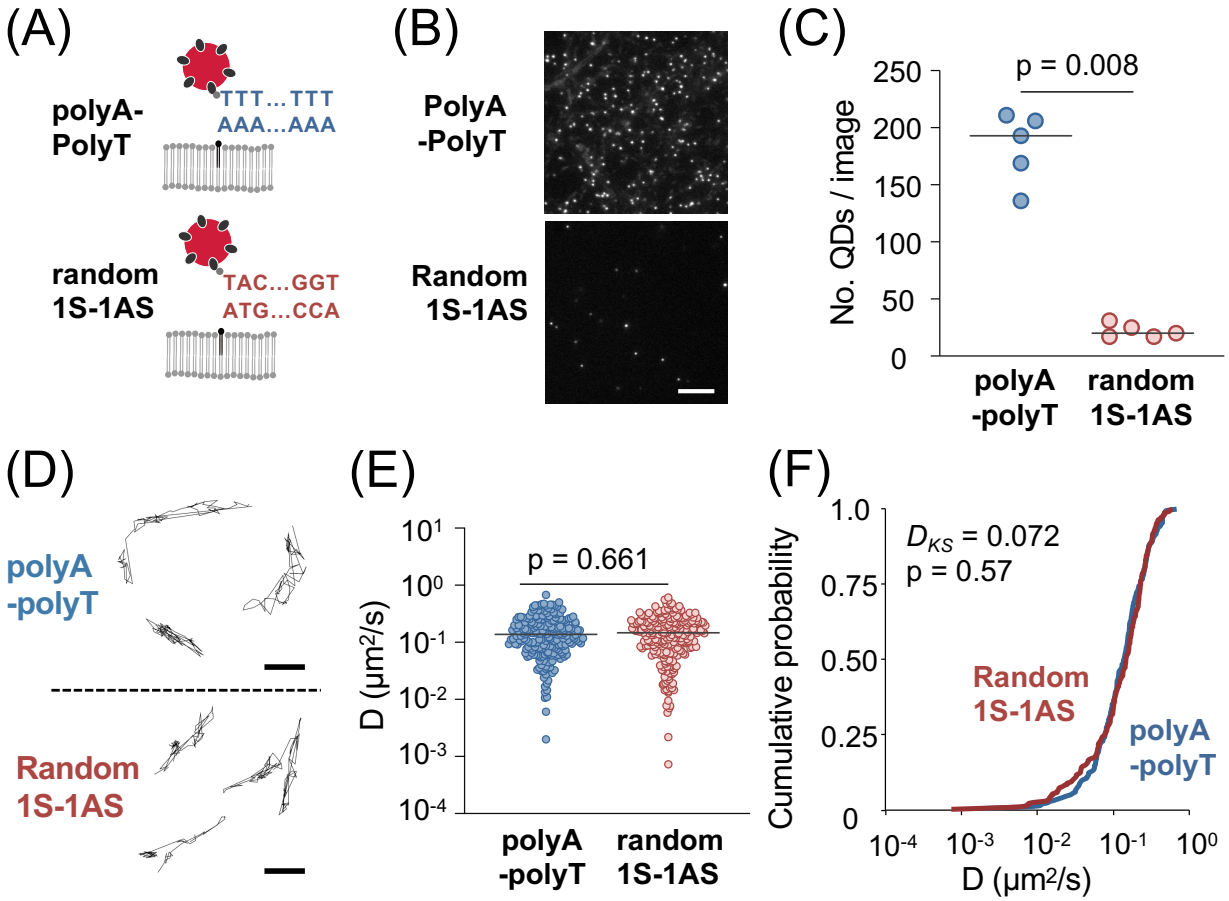
(A)
polyA-
PolyT
TTT...TTT
AAA...AAA
random
1S-1AS
TAC...GGT
ATG...CCA
(B)
PolyA
-PolyT
Random
1S-1AS
(C)
p = 0.008
No. QDs / image
250
200
150
100
50
0
polyA
-polyT
random
1S-1AS
(D)
polyA
-polyT
Random
1S-1AS
(E)
p = 0.661
D (μm²/s)
10¹
10⁰
10⁻¹
10⁻²
10⁻³
10⁻⁴
polyA
-polyT
random
1S-1AS
(F)
Cumulative probability
1.0
0.75
0.50
0.25
0
D_KS = 0.072
p = 0.57
Random
1S-1AS
polyA
-polyT
10⁻⁴
10⁻³
10⁻²
10⁻¹
10⁰
D (μm²/s)

Figure 4

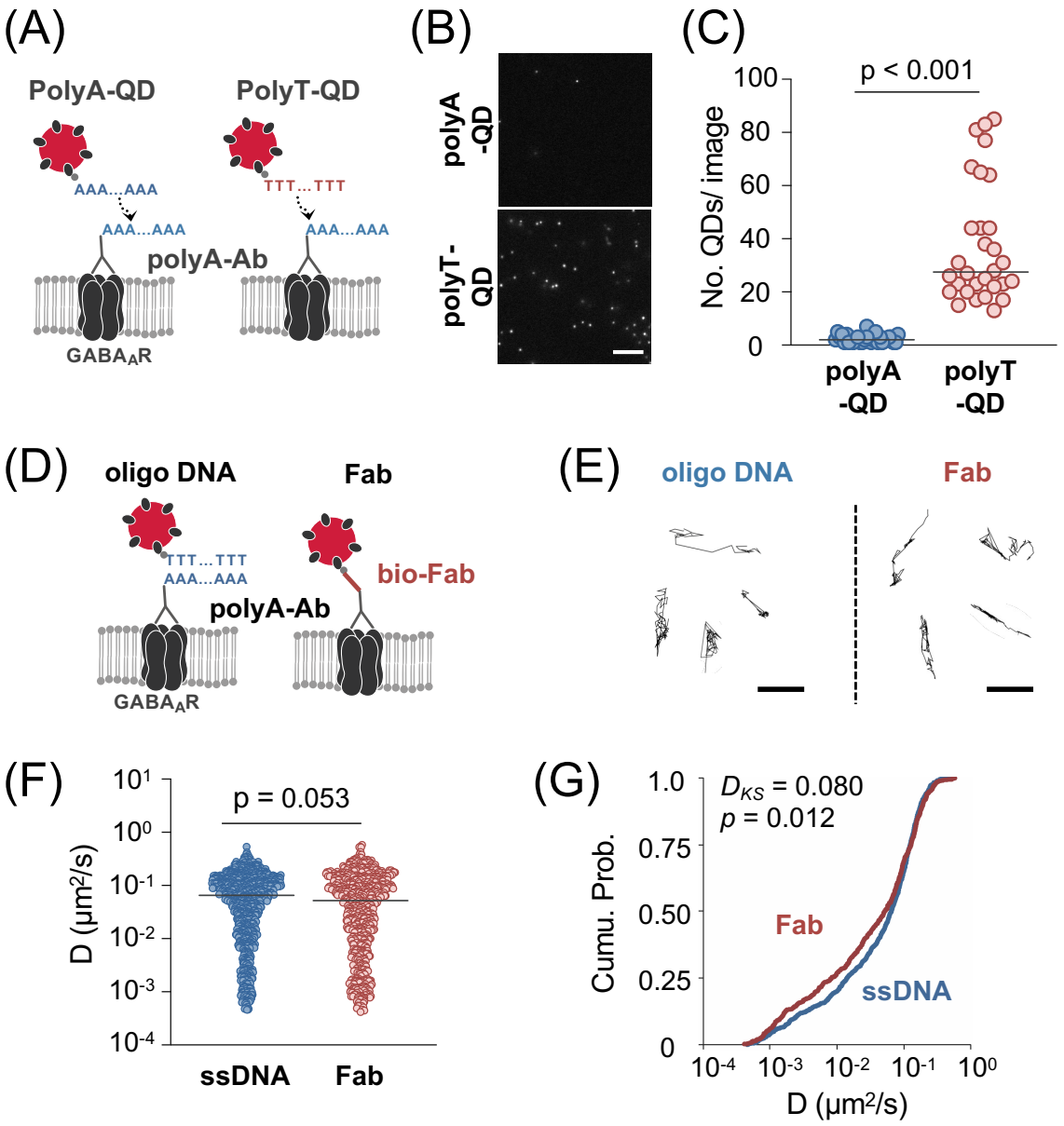
(A)
PolyA-QD
PolyT-QD
AAA...AAA
TTT...TTT
AAA...AAA
AAA...AAA
polyA-Ab
GABA$_A$R
(B)
polyA -QD
polyT- QD
(C)
p < 0.001
No. QDs/ image
100
80
60
40
20
0
polyA -QD
polyT -QD
(D)
oligo DNA
Fab
TTT...TTT
AAA...AAA
bio-Fab
polyA-Ab
GABA$_A$R
(E)
oligo DNA
Fab
(F)
p = 0.053
D (μm²/s)
10^1
10^0
10^{-1}
10^{-2}
10^{-3}
10^{-4}
ssDNA
Fab
(G)
D_{KS} = 0.080
p = 0.012
Cumu. Prob.
1.0
0.75
0.50
0.25
0
Fab
ssDNA
10^{-4}
10^{-3}
10^{-2}
10^{-1}
10^0
D (μm²/s)

Figure 5

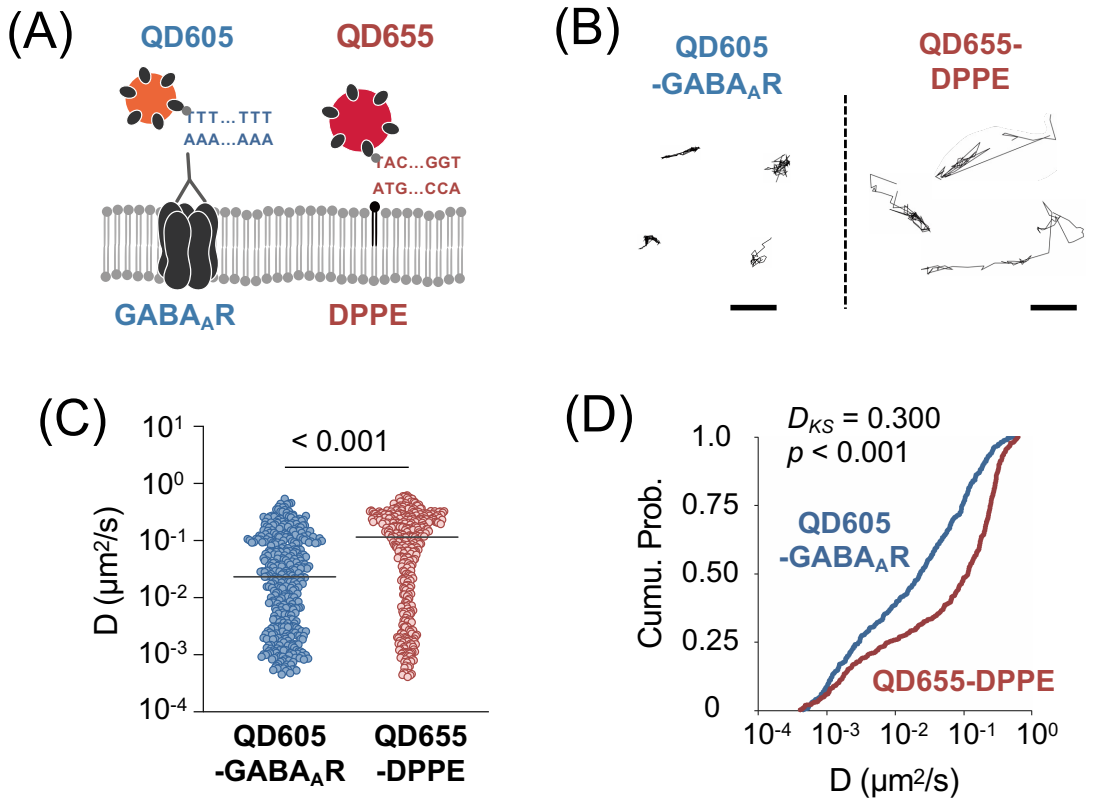
(A)
QD605
QD655
TTT...TTT
AAA...AAA
TAC...GGT
ATG...CCA
GABA$_A$R
DPPE
(B)
QD605
-GABA$_A$R
QD655-
DPPE
(C)
< 0.001
D (μm²/s)
QD605
-GABA$_A$R
QD655
-DPPE
(D)
D_{KS} = 0.300
p < 0.001
Cumu. Prob.
QD605
-GABA$_A$R
QD655-DPPE
D (μm²/s)

Figure6

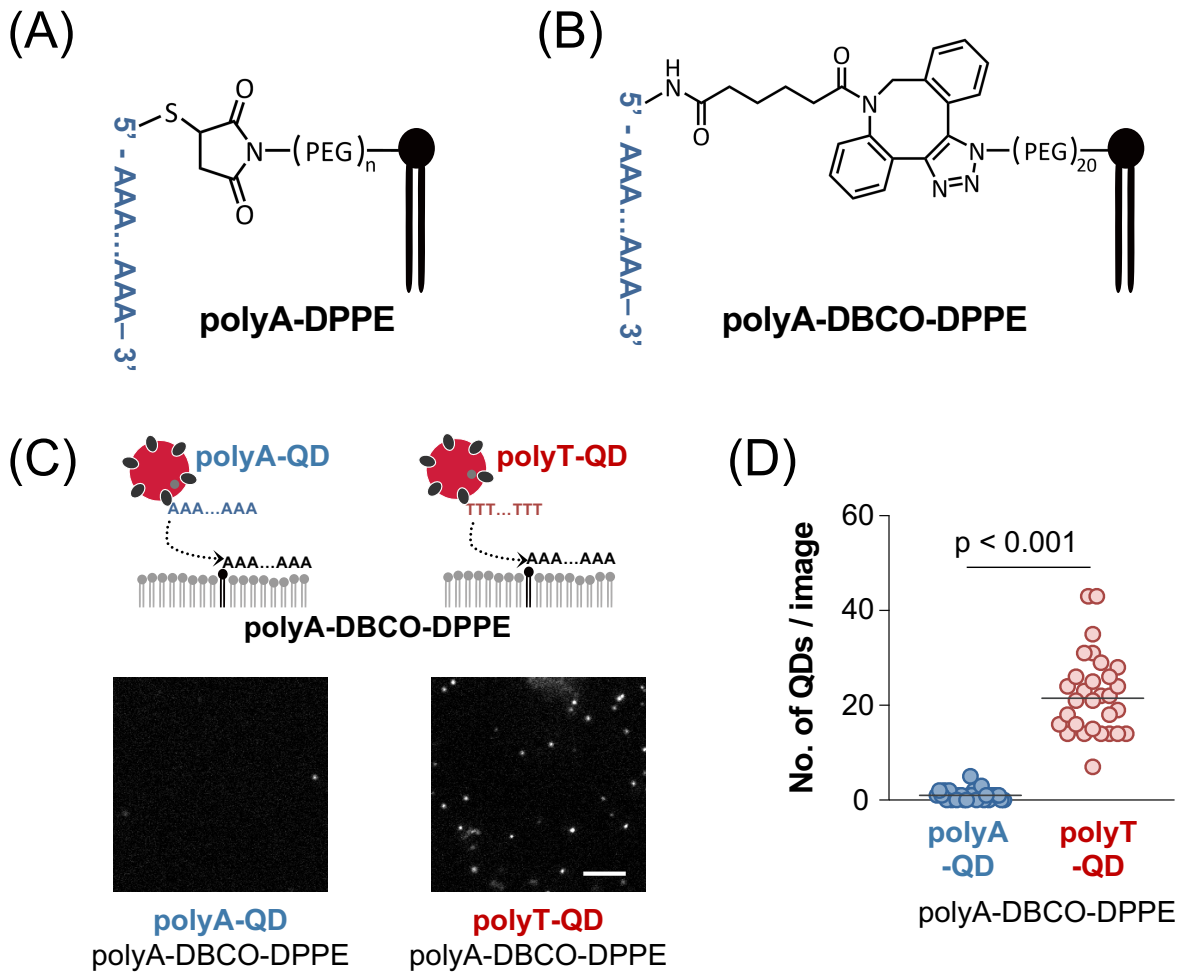

Supplementary Figure S1

Effect of the linker between DPPE and ssDNA on the specificity of QD labeling
(A) DPPE fused to polyA ssDNA via a thiol–maleimide reaction (polyA–DPPE), and (B) DPPE fused to polyA ssDNA via click chemistry using dibenzocyclooctyl (DBCO)–azide conjugation (polyA–DPPE–DBCO). (C) QD images polyA–DPPE–DBCO targeted with polyA–QD (left) and polyT–QD (right). Scale bar indicates 10 µm. (C) Number of QDs per field of view with median (solid lines). N = 29 images for polyA–QD, N = 30 images for polyT.

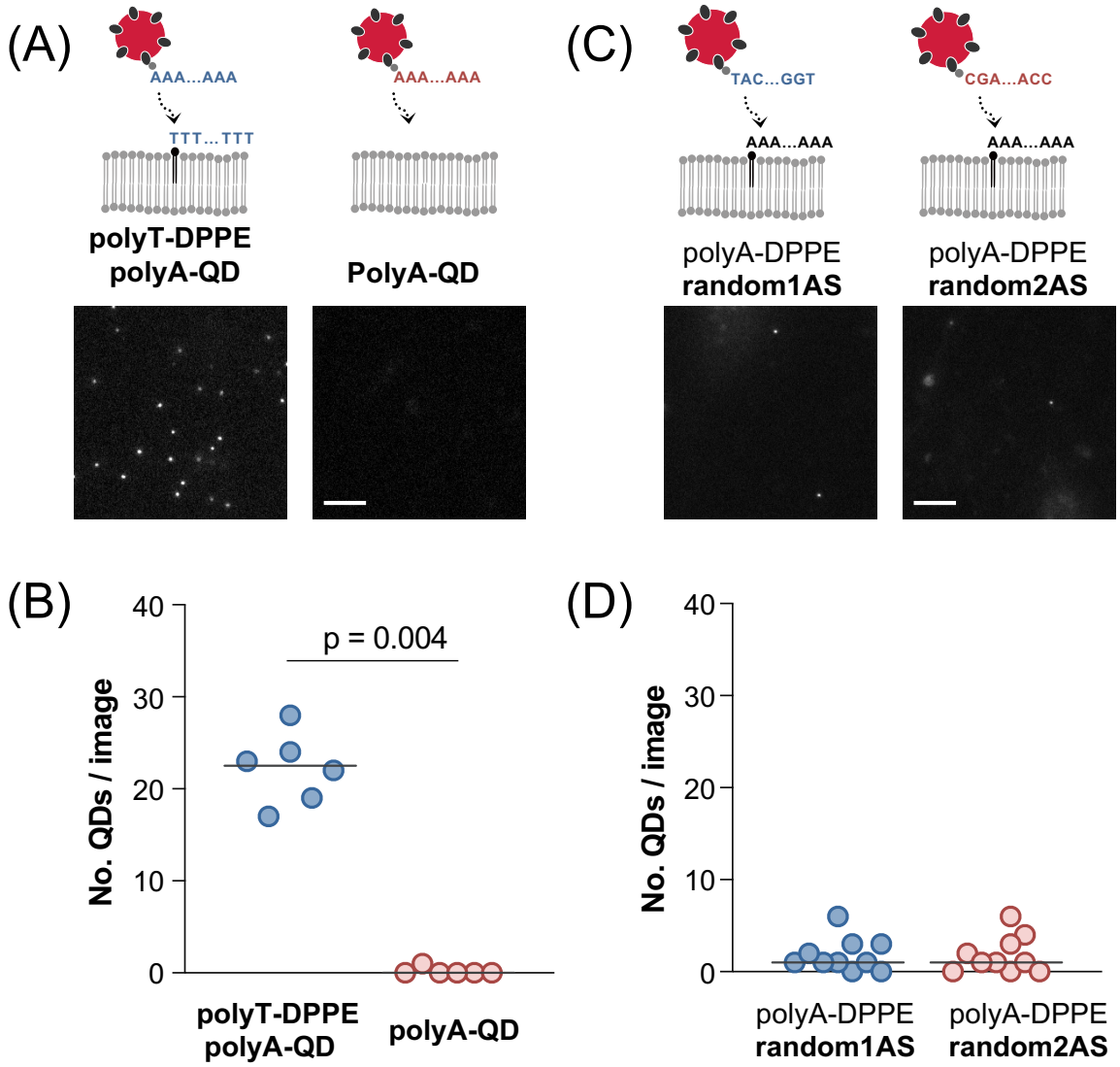

Supplementary Figure S2

Specificity of ssDNA–QD binding to the DPPE

(A) (B) Representative QD images for polyA–QD targeted to the neurons with (left) or without (right) polyT–DPPE (A) and the number of QDs per field of view (B). The black line indicates the median.

(C) (D) QD images of neurons with polyT–DPPE targeted with QDs with two random sequences (C), and the number of QDs per field of view (D). Scale bars indicate 10 μm. Bars in the dot plots indicate the median.

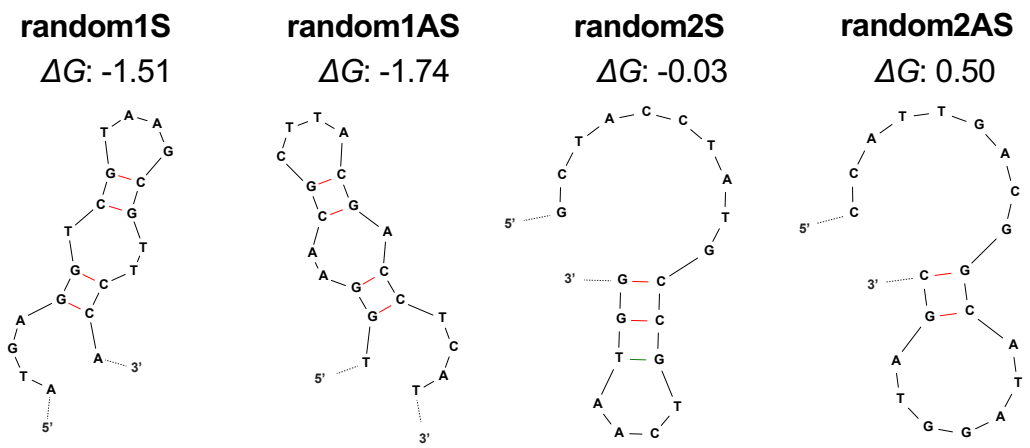

Supplementary Figure S3

Secondary structures predicted by mfold [33] for the random ssDNAs used in this experiment. Red lines indicate canonical base pairs of Watson–Crick type, which contribute significantly to the thermodynamic stability of the structure. Green lines indicate non-canonical or weak base pairing; ΔG denotes free energy change [kcal/mol].